

Real-time monitoring energy efficiency and performance degradation of condensing boilers

Baldi, Simone; Le, Thuan; Holub, Ondrej; Endel, P.

DOI

[10.1016/j.enconman.2017.01.016](https://doi.org/10.1016/j.enconman.2017.01.016)

Publication date

2017

Document Version

Final published version

Published in

Energy Conversion and Management

Citation (APA)

Baldi, S., Le, T., Holub, O., & Endel, P. (2017). Real-time monitoring energy efficiency and performance degradation of condensing boilers. *Energy Conversion and Management*, 136, 329-339. <https://doi.org/10.1016/j.enconman.2017.01.016>

Important note

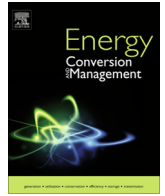
To cite this publication, please use the final published version (if applicable). Please check the document version above.

Copyright

Other than for strictly personal use, it is not permitted to download, forward or distribute the text or part of it, without the consent of the author(s) and/or copyright holder(s), unless the work is under an open content license such as Creative Commons.

Takedown policy

Please contact us and provide details if you believe this document breaches copyrights. We will remove access to the work immediately and investigate your claim.



Real-time monitoring energy efficiency and performance degradation of condensing boilers



Simone Baldi^{a,*}, Thuan Le Quang^{a,c}, Ondrej Holub^b, Petr Endel^b

^a Delft Center for Systems and Control, Delft University of Technology, Delft 2628CD, The Netherlands

^b Honeywell Prague Laboratory, V Parku 2326/18, 148 00 Prague 4, Czech Republic

^c Department of Mathematics, Quy Nhon University, Viet Nam

ARTICLE INFO

Article history:

Received 16 September 2016

Received in revised form 6 January 2017

Accepted 6 January 2017

Available online 19 January 2017

Keywords:

Condensing boilers

Real-time performance monitoring

Mass flow virtual sensor

Fault detection and diagnosis

ABSTRACT

Condensing boilers achieve higher efficiency than traditional boilers by using waste heat in flue gases to preheat cold return water entering the boiler. Water vapor produced during combustion is condensed into liquid form, thus recovering its latent heat of vaporization, leading to around 10–12% increased efficiency. Many countries have encouraged the use of condensing boilers with financial incentives. It is thus important to develop software tools to assess the correct functioning of the boiler and eventually detect problems. Current monitoring tools are based on boiler static maps and on large sets of historical data, and are unable to assess timely loss of performance due to degradation of the efficiency curve or water leakages. This work develops a set of fault detection and diagnosis tools for dynamic energy efficiency monitoring and assessment in condensing boilers, i.e. performance degradation and faults can be detected using real-time measurements: this real-time feature is particularly relevant because of the limited amount of data that can be stored by state-of-the-art building energy management systems. The monitoring tools are organized as follows: a bimodal parameter estimator to detect deviations of the efficiency of the boiler from nominal values in both condensing and noncondensing mode; a virtual sensor for the estimation of the water mass flow rate; filters to detect actuator and sensor faults, possibly due to control and sensing problems. Most importantly, structural properties for detection and isolation of actuators and sensing faults are given: these properties are crucial to understand which faults can be diagnosed given the available measurements. The effectiveness of these tools is verified via extensive simulations.

© 2017 The Author(s). Published by Elsevier Ltd. This is an open access article under the CC BY license (<http://creativecommons.org/licenses/by/4.0/>).

1. Introduction

Building energy use, mainly driven by heating, ventilating and air conditioning (HVAC) equipment, is responsible for over a third of Europe and US global energy consumption and CO₂ emissions which are supposed to heavily contribute to climate change [1]. In order to achieve higher energy efficiency levels, a range of technical solutions must not only help building professionals in selecting and installing the most suitable heating systems, but also constantly monitor them, using fault detection and diagnosis tools [2]. Monitoring techniques give the possibility, when properly

developed, to improve energy efficiency, decrease running costs and reduce emissions [3].

While most of the techniques used in fault detection and diagnosis for building automation purposes are based on steady-state reasoning (i.e. dynamic heat transfer behavior is often neglected), the purpose of this work is to explore the possibility of including *dynamical models for fault detection and diagnosis purposes*. It has to be underlined that current state-of-the-art monitoring tools are based of static maps of the equipment, and in order to assess loss of performance it is necessary to have large sets of historical data to be used to benchmark performance of different period in the life time of the equipment. It is thus of practical importance to develop tools that can use data in real-life and possibly detect performance changes timely: this can potentially be achieved by developing monitoring tools based on dynamic models of the HVAC equipment. Including dynamical models in monitoring is crucial to distinguish, in real-time HVAC system operation, among the following possibilities for loss of performance:

* Corresponding author.

E-mail addresses: s.baldi@tudelft.nl (S. Baldi), lethuan2004@yahoo.com (T.L. Quang), Ondrej.Holub@Honeywell.com (O. Holub), Petr.Endel@Honeywell.com (P. Endel).

- (a) Different working points.
- (b) Incipient faults (parameter drift).
- (c) Faults in the controller.

The focus of this work is on the condensing boiler case, because this kind of equipment is becoming more and more adopted. The relevance of the condensing boiler case arises from the fact that, with respect to the total HVAC operation, boilers are estimated to contribute to 85% of the energy consumption and 67% of the CO₂ emissions [4]. The temperature of the flue gas exiting a traditional boiler is usually high, so that a great amount of heat is lost to the environment. Condensing boilers aim at recovering sensible and latent heat of the flue gas by adding a condensing heat exchanger (see Fig. 1). The condensing heat exchanger uses the return water as the cooling medium. When the return temperatures from the heating system is sufficiently low (below the dew temperature of the flue gas) the latent heat of water vapor in the flue gas can be recovered, so as to achieve significantly higher efficiency than traditional boilers. The key point is maintaining a high difference between supply and return temperature. When this condition is not maintained, the boiler will operate in a non condensing mode [5]. Due to its typical bimodal behavior (condensing, noncondensing mode), fault detection and diagnosis in condensing boilers is challenging and still not fully explored. To the best of the authors' knowledge, no dynamic monitoring tools have been developed specifically for condensing boilers: most static fault detection techniques for condensing boilers are based on checking the difference between the supply water temperature set-point and the actual supply water temperature¹ [6].

It is relevant to consider the dynamics of the boiler (as opposed to steady-state static behavior) because dynamics can take into account transient behavior in the temperature profile. Dynamic behavior is crucial since the condensing boiler presents all the aforementioned three possibilities (a)–(c) for loss of performance (which should be distinguished from each other for a proper diagnosis of the problem):

- (a) *Different working points*: the boiler has a nonlinear efficiency curve (depending on the boiler power and/or the return water temperature). The efficiency curve is often described with a (piecewise) polynomial curve in these variables.
- (b) *Incipient faults (parameter drift)*: incrustation and corrosion cause slowly decreasing degradation of performance, whose trend is important to identify, so as to take appropriate maintenance actions.
- (c) *Faults in the controller*: the boiler includes a burner controller regulating the supply temperature: for example, the burner might stop functioning or function at reduced power. If not working properly, such faults must be timely and correctly diagnosed.

1.1. Related work

Condensing boilers are equipped with two heat exchangers, a primary (dry) heat exchanger and a secondary (wet) heat exchanger. An optimal design of heat exchangers can lead to heating efficiency of about 90% when using the optimal designed heat exchangers. Compared to a conventional Bunsen-type boilers, the heating efficiency can be improved of about 10% [7]. Special pre-burners (that mix and preburn air and gas) can also increase efficiency and reduce emissions [8]. The development of new types

¹ A typical static technique is based on checking whether a desired temperature set point is reached at steady state. This static technique might result in false alarms if transient behavior occurring during operation, maintenance actions or replacement of boiler with a new one, is not taken into account.

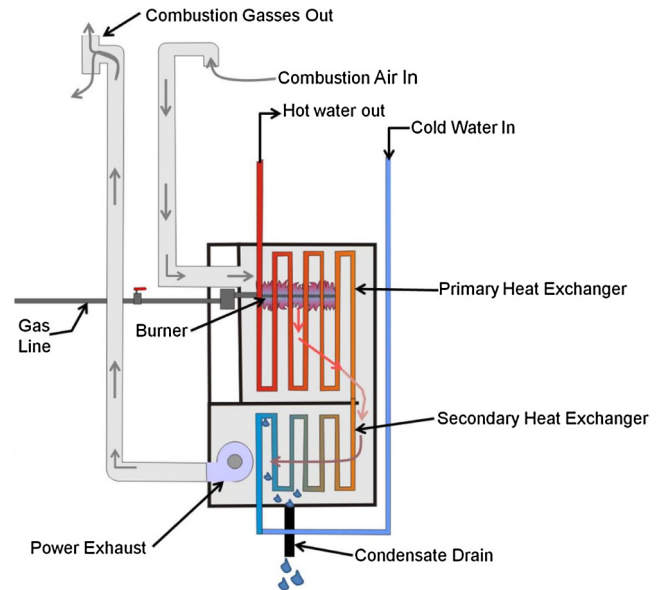


Fig. 1. Condensing boiler (source: U.S. Department of Energy).

of boilers with higher efficiency and lower emissions is an active area of research, e.g. exhaust gas recirculation-condensed water recirculation-waste heat recovery condensing boilers (EGR-CWR-WHR CB) [9], with an efficiency of almost 94%. Traditional natural gas fired boiler can be retrofitted into condensing boilers as soon as the return temperature, which varies with the seasonal ambient temperature, is lower than the dew temperature of the flue gas during most of a heating season [10]. Condensing boilers can be adopted not only for residential applications, but they are becoming widespread in process industry [11] and district heating systems [12].

The development of analytical boiler models is at the base of optimal boiler design and monitoring [13]: in [14] a simple model was developed to predict that the seasonal efficiency of condensing boilers based on the efficiency at full load evaluated at return water mean temperature. In [15] a heat and mass transfer analytical model of a condensing heat exchanger system was developed so as to predict the heat transferred from flue gas to cooling water and the condensation rate of water vapor in the flue gas. The main purpose of these models is to predict the boiler efficiency according to certain design parameters choices. In fact, the use of these models allows the computation of relevant variables like flue gas exit temperature, supply water temperature, water vapor mole fraction, and condensation rate of water vapor [16]. However, to the best of the authors' knowledge these models have never been used for real-time dynamic fault detection and diagnosis purposes. Furthermore, when considering condensing boilers, an important issue is related to the dynamic estimation of non accessible quantities like mass flows: sensors to measure mass flow can be quite elaborate and expensive [17], and are available in almost no commercial boiler). Monitoring mass flow rate is an important part of monitoring tools, because it allows to detect degradation due to limescale deposit in boiler pipes, or leakages [18]. In order to advance the state of the art, this work is the first one, to the best of the authors' knowledge exploiting boiler dynamics for the design of advanced virtual sensing and fault detection and diagnosis tools. The tools are organized as follows: a bimodal parameter estimator to detect deviations of the efficiency of the boiler from nominal values in both condensing and noncondensing mode; a virtual sensor for the estimation of the water mass flow rate; filters to detect actuator and sensor faults, possibly due to control and sensing problems.

1.2. Condensing boiler operation

In this work the boiler is considered to operate so as to track a certain supply temperature. Thermostatic radiator valves (TRVs), weather compensation, optimized start/stop are nowadays implemented by controllers [19], that will decide at every time, the most suitable set point for the supply water temperature. Consider a condensing boiler that responds to the temperature set point via a *modulating burner*. In fact, almost all boilers nowadays have modulating burners which control the output of the burner to match the requested load [20]. An embedded logic determines whether the boiler should step on or step down the gas: this logic is typically based on the feedback from water temperature in supply and return pipes. When the temperature difference between supply and return increases, more heat is requested by the building and the boiler steps on the gas. As the temperature difference decreases, the gas is stepped down.

Boiler operation is only one part of a bigger control system (energy management system) that regulates energy supply and demands in buildings [21]: these management and control systems are typically composed of two layers. At the upper layer, advanced control strategies are in charge of deciding the set points according to which each piece of HVAC equipment should run (e.g. supply water for boilers, water velocity for pumps, air velocity for fans, thermostats set points) to achieve energy efficiency or even demand response functionalities: in [22] model predictive control is used to manage the demand of a microgrid with controllable loads; in [23] a game-theoretic approach is to shave energy peaks of residential customers; the authors of [24] use a multi-agent control system to control building indoor energy and comfort; by using rule-based strategies, the work [25] shows energy efficiency in an apartment public housing complex by aligning the distribution of residents' thermostat preferences with the indoor temperature; [26] attains reduced operational costs for six apartments with HVAC systems controlled via a genetic algorithm; [26] attains reduced operational costs for six apartments with HVAC systems controlled via different configurations; a genetic algorithm in [27] controls the HVAC system of a building floor to insure comfort and indoor air quality with reduced energy consumption; Tabu search is used in [28] to balance the fluctuating power supply from renewable energy with the demand of apartment houses; the authors in [29] use adaptive optimization to decide the optimal thermostat set point to balance demand and thermal comfort. At the lower layer, a bank of PID controller operates each piece of HVAC equipment so as to attain the set point (e.g. operate the burner to achieve the desired boiler supply temperature, drive the current/voltage of pumps and fans motors to achieve desired speed, operate valve radiators to achieve thermostats set points). Different banks of PID have been proposed in literature, whose operation usually depends on external factors like outside temperature or user preferences: fuzzy adaptive comfort temperature is proposed in [30] for the intelligent climate control; [31] illustrates the use of fuzzy reasoning for improving the fuzzy HVAC control performance depending on comfort of the inhabitants; in [32] a finite-difference method adjusts HVAC operation mode based on the influence of all possible thermal loads in conjunction with thermal comfort requirements; a physics-based optimization is used in [33] for multivariable PID control of HVAC components; to conclude this overview, the review paper [34] also discusses data-driven optimization for PID control of HVAC components. It has to be noted that all the aforementioned low-level and upper-level control layers always assume perfect operation of the HVAC equipment: the proposed monitoring tools can be adopted (in real-time) by upper-level control layers to recalculate the optimal energy generation taking into account degradation of the HVAC equipment [35].

The rest of the paper is organized as follows: Section 2 gives the basics of boiler functioning and of possible faults and problems that might occur during operation. Section 3 develops a bimodal estimation method to monitor boiler efficiency and mass flow. Section 4 focuses on detecting actuator faults: there, fundamental limitations for detectability and isolability of faults are given. By relaxing detectability and isolability conditions, Section 5 develops two Kalman-filter based residual generators for detecting and isolating actuator and sensor faults. Section 6 tests the proposed methods via extensive simulations. Section 7 concludes the work. Nomenclature is given in Table 1.

2. Boiler degradation and faults

This section is meant to give the basics of boiler functioning and of possible faults and problems that might occur during operation. The efficiency of the boiler is the main factor in the overall efficiency of a domestic/commercial central heating system. Minimum standards of efficiency are required by law for most boiler types. In most countries, it is now a requirement of the building regulations that newly installed gas-fired boilers should be condensing with a seasonal efficiency of 85% or more [36]. The efficiency of the overall system has a major impact on running costs and the associated CO₂ and NO_x emissions. Among other factors, boiler efficiency depends upon:

- Fuel (oil, natural gas).
- Boiler and heat exchanger design.
- Inlet and outlet temperatures.
- Load requested to the boiler.
- Burner control (on/off, air/gas modulating).
- Presence of scale.
- Regular maintenance.

Let us now examine the main faults that might cause changes in the boiler efficiency curve. Extremely cold winter weather can shut down the boiler if the *condensate pipe* freezes. In fact, the condensate leaves the boiler through an outlet pipe which is sometimes placed outside the building so as to connect to the waste water system. If cold temperatures freeze the condensate in the pipe a blockage might happen, which will cause the boiler to shut down: this can be regarded as an actuator fault, which has to be detected and diagnosed by the monitoring tools. Also temperature sensors might give wrong measurements due to faults: as a result, sensor faults have also to be detected and diagnosed.

Another common problem is *limescale*, which can build up on the water pipes of the heat exchanger and create an insulating layer which inhibits heat transfer to the water. It has been calculated that a 1 mm layer of limescale causes a 7% increase in boiler energy to meet the same heat demand, thus significantly modifying the boiler efficiency curve [37]. Another problem to be considered is the following: the plates of a boiler never get hotter than the water when in contact with it, whatever may be the outside temperature applied. When coated with scale, and thus removed from direct contact with water, boiler plates get so overheated as to rapidly deteriorate in quantity and quality. But the cost due to this incrustation is not its chief disadvantage – it is a source of positive danger. When the scale gets thick, and the plates consequently very hot, the former is liable to crack off, bringing the water in contact with over-heated metal, and thereby causing explosions. These phenomena can be regarded as a combination of degradation of the boiler efficiency curve and changes in the mass flow rate, which have to be detected and diagnosed by the monitoring tools.

Furthermore, as boiler *insulation* degrades, heat losses as high as 10% can occur [37]. Insulation should be replaced over time when

Table 1

Nomenclature. In addition to these symbols, the notation T^{eq}, P^{eq} indicates an equilibrium value, and \bar{T}, \bar{P} a deviation from the equilibrium.

| Explanation | Symbol | Unit |
|-------------------------------------|-------------|----------------------|
| Boiler supply water temperature | T_{sw} | [°C] |
| Boiler supply water temp. (layer 1) | T_{sw_1} | [°C] |
| Boiler supply water temp. (layer 2) | T_{sw_2} | [°C] |
| Boiler supply water temp. (layer 3) | T_{sw_3} | [°C] |
| Boiler return water temperature | T_{rw} | [°C] |
| Boiler power (gas side) | P_{in} | [kW] |
| Boiler power (water side) | P_{out} | [kW] |
| Boiler efficiency | η | [-] |
| Water mass flow rate | m_w | [kg/s] |
| Specific heat of water | c_w | [kJ/kg °C] |
| Density of water | ρ_w | [kg/m ³] |
| Volume of boiler | V_b | [m ³] |
| Volumetric gas flow rate | \dot{V}_g | [m ³ /s] |
| Gas heating value | H_v | [kJ/m ³] |
| Actuator fault | f_a | [kW] |
| Sensor fault | f_s | [°C] |

it is showing signs of wear. Surely, loss of insulation will lead to a degradation of the boiler efficiency curve, which has to be detected and diagnosed. A more complete list of boiler faults can be found at [38].

3. Monitoring boiler efficiency and mass flow

To obtain higher efficiency than traditional boilers, in condensing boilers the water vapor in the exhaust gas is condensed and the latent heat that is released and used to preheat the return water. The colder the return water temperature, the greater the amount of water vapor that can be condensed. Consequently, achieving higher boiler efficiency requires returning water to the boiler at a temperature below the dew temperature (56 °C for flue gases²). Below the dew temperature, the water vapor changes phase to liquid; above the dew temperature, the water vapor entrained in flue products remains vaporized, and the condensing boiler will operate with reduced heat recovery. Fig. 2 shows, in a typical condensing boiler, the efficiency curve against the return temperature: the inflexion point visible in the curve at around 56 °C indicates that the dew point temperature is reached and from there the efficiency improvement is very rapid.

As a result of Fig. 2, the boiler exhibits a bimodal efficiency curve. The efficiency of a boiler must be checked in real-time, since boiler efficiency usually deteriorates with age due to degradation and wear and tear. The efficiency of a boiler is modeled as:

$$P_{out} = \eta(P_{in}, T_{rw}, \vartheta)P_{in} \quad (1)$$

where P_{in} is the consumed power in terms of gas (i.e. the power paid on the gas bill) and which can be directly measured, P_{out} is the generated power, i.e. the power delivered to the water, and T_{rw} is the temperature of the return water. In (1) $\eta(P_{in}, T_{rw}, \vartheta)$ (where ϑ is a set of parameters to be identified) is the efficiency curve of the boiler which is assumed to be a piecewise function in P_{in} and T_{rw} , i.e.

$$\eta(P_{in}, T_{rw}, \vartheta) = \begin{cases} \vartheta_0^c + \vartheta_1^c P_{in} + \vartheta_2^c T_{rw} + \vartheta_3^c T_{rw} P_{in} + \vartheta_4^c T_{rw}^2 & \text{if } T_{rw} \leq 56^\circ\text{C} \\ \vartheta_0^{nc} + \vartheta_1^{nc} P_{in} + \vartheta_2^{nc} T_{rw} & \text{if } T_{rw} > 56^\circ\text{C} \end{cases} \quad (2)$$

where the superscripts *c* and *nc* stand for the condensing and non-condensing modes, respectively. The meaning of the model (2) is the following: first, it is composed of two functions in order to

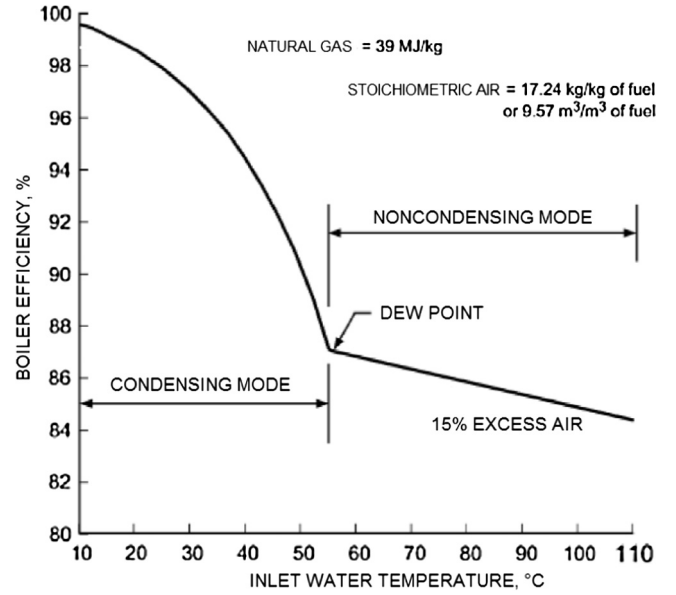


Fig. 2. Effect of return (inlet) temperature on efficiency of condensing boilers [39].

account for the boiler bimodal behavior; second, both functions are linear in P_{in} (in particular, we expect the efficiency to decrease linearly as P_{in} increases); thirdly, the first function is quadratic in T_{rw} , while the second function is linear in both T_{rw} (cf. the parabola-like curve and straight line curve in Fig. 2). The model (2) is based on experimental data, as explained in [40]. Let us rewrite (2) in a more compact form as

$$\eta(P_{in}, T_{rw}, \vartheta) = \begin{cases} \vartheta^c \phi(P_{in}, T_{rw}) & \text{if } T_{rw} \leq 56^\circ\text{C} \\ \vartheta^{nc} \phi(P_{in}, T_{rw}) & \text{if } T_{rw} > 56^\circ\text{C} \end{cases} \quad (3)$$

where

$$\vartheta^c = [\vartheta_0^c \ \vartheta_1^c \ \vartheta_2^c \ \vartheta_3^c \ \vartheta_4^c]'$$

$$\vartheta^{nc} = [\vartheta_0^{nc} \ \vartheta_1^{nc} \ \vartheta_2^{nc} \ 0 \ 0]'$$

$$\phi(P_{in}, T_{rw}) = [1 \ P_{in} \ T_{rw} \ T_{rw}P_{in} \ T_{rw}^2] \quad (4)$$

Apparently, the total number of parameters to be identified in (3) is eight: however, since the two functions in (3) must be continuous in $T_{rw} = 56^\circ\text{C}$, we have $\vartheta^c \phi(P_{in}, 56) = \vartheta^{nc} \phi(P_{in}, 56), \forall P_{in}$, which leads to two equality constraints

$$\vartheta_0^c - \vartheta_0^{nc} + 56(\vartheta_2^c - \vartheta_2^{nc}) + 56^2 \vartheta_4^c = 0$$

$$\vartheta_1^c - \vartheta_1^{nc} + 56 \vartheta_3^c = 0 \quad (5)$$

thus resulting in six independent parameters instead of eight. A more convenient way is to write (3) in the max-form [41]

$$\eta(P_{in}, T_{rw}, \vartheta) = \vartheta^c \phi(P_{in}, T_{rw}) - h \max\{c' \phi(P_{in}, T_{rw}), 0\} \quad (6)$$

where $h \in \mathbb{R}$ is a scalar vector parameter to be identified and $c = [-56 \ 0 \ 1 \ 0 \ 0 \ 0]'$. The max-form (6) comprises all the six parameters to be estimated.

It results that the efficiency relation can be written as

$$\eta(P_{in}, \theta) = \bar{\vartheta}' \bar{\phi}(P_{in}, T_{rw}) \quad (7)$$

where

$$\bar{\vartheta} = \begin{bmatrix} \vartheta^c \\ h \end{bmatrix}, \quad \bar{\phi}(P_{in}, T_{rw}) = \begin{bmatrix} \phi(P_{in}, T_{rw}) \\ \max\{c' \phi(P_{in}, T_{rw}), 0\} \end{bmatrix} \quad (8)$$

² The dew point is calculated for 3% oxygen and 15% excess of air, optimal values for condensing boilers. In this study these values are assumed to be kept constant by the air/fuel inlet control system.

Remark 1. Note that (7) is a linear-in-the-parameters model. This is a very important feature that will allow the development of an efficient estimator. Furthermore, notice that the max-form (6) requires only six parameters to be estimated, in contrast with the eight parameters in (2). The reduction of parameters via achieved via the continuity condition of the efficiency curve. Thus, (6) is a minimal form with respect to the parameters to be identified, and this will make the estimator convergence faster.

The next step is embedding (7) in the boiler dynamic model which describes the heat and mass transfer

$$\begin{aligned} c_w \rho_w V_b \dot{T}_{sw}(t) &= P_{out}(t) - c_w m_w(t)(T_{sw}(t) - T_{rw}(t)) \\ P_{in}(t) &= \dot{V}_g(t) H_v(t) \end{aligned} \quad (9)$$

where c_w is the specific heat of water, ρ_w the water density, V_b the volume of the boiler, m_w is the mass flow of water, \dot{V}_g is the gas volumetric flow and H_v is the heating value for volume. In (9) T_{sw} represents the supply water temperature, and T_{rw} represents the return water temperature flowing into the boiler. The model (9) is a dynamic model that describes the fact that the change in temperature of the water in a boiler is given by the heat supplied and the difference between supply and return water temperature. Note that it is assumed that the supply water has the same temperature T_{sw} as the water inside the boiler. This is a simplification that often works in practice. A more realistic model one possibility could be derived by dividing the boiler into layers, where each layer exchanges heat with the others according to relations similar to (9) [34]. The dynamic model (9) can be written in the special bilinear form

$$z = \rho^*(\bar{\vartheta}^* \bar{\varphi} + z_0) \quad (10)$$

after filtering (9) on the left a right-hand side via a stable filter

$$c_w \rho_w V_b \frac{s \lambda T_{sw}}{s + \lambda}(t) = \frac{\bar{\vartheta}' \bar{\varphi}(P_{in}(t), T_{rw}(t)) P_{in}(t)}{s + \lambda} - \frac{c_w m_w(t)(T_{sw}(t) - T_{rw}(t))}{s + \lambda}$$

where $\lambda > 0$ is the stable pole of the filter, we obtain

$$c_w \rho_w V_b \lambda T_{sw_d}(t) = \bar{\vartheta}' \bar{\varphi}(P_{in}(t), T_{rw}(t)) P_{in_f}(t) - c_w m_w(t)(T_{sw_f}(t) - T_{rw_f}(t)) \quad (11)$$

where

$$\begin{aligned} T_{sw_d}(t) &= \frac{s \lambda T_{sw}}{s + \lambda} T_{sw}(t), & P_{in_f}(t) &= \frac{\lambda T_{rw}}{s + \lambda} P_{in}(t) \\ T_{sw_f}(t) &= \frac{\lambda T_{rw}}{s + \lambda} T_{sw}(t), & T_{rw_f}(t) &= \frac{\lambda T_{rw}}{s + \lambda} T_{rw}(t) \end{aligned}$$

are filtered measurements. In (11) the following assumptions are taken

A 1. c_w , ρ_w , V_b are known and P_{in} , T_{sw} and T_{rw} can be measured, which are measures and information available in most boilers.

A 2. Consequently, T_{sw_d} , T_{sw_f} , T_{rw_f} and P_{in_f} can be calculated from filtered measurements, while $\bar{\vartheta}$ and m_w must be estimated in real-time: in fact, in most commercial boilers there are no sensors that can provide this information.

A 3. Furthermore, assume that the mass flow rate m_w is almost constant or slowly varying (and different than zero).

Under assumptions A1–A3, divide (11) by $m_w(t)$ so as to obtain

$$c_w(T_{sw_f}(t) - T_{rw_f}(t)) = \frac{1}{m_w(t)} \left(\bar{\vartheta}' \bar{\varphi}(P_{in}(t), T_{rw}(t)) P_{in_f}(t) - c_w \rho_w V_b \lambda T_{sw_d}(t) \right) \quad (12)$$

which has the same form as (10), with

$$\begin{aligned} z(t) &= c_w(T_{sw_f}(t) - T_{rw_f}(t)) \\ z_1(t) &= -c_w \rho_w V_b \lambda T_{sw_d}(t) \\ \rho^* &= \frac{1}{m_w(t)} \\ \bar{\varphi} &= \bar{\varphi}(P_{in}(t), T_{rw}(t)) P_{in_f}(t) \end{aligned} \quad (13)$$

3.1. Online estimation of efficiency and mass flow

One task of performance monitoring is estimating the efficiency curve of the boiler at each time step, based on observations. Similarly, the mass flow must be estimated because there are no measurements available for it: consider the estimation error

$$\begin{aligned} \hat{z} &= \rho(\bar{\vartheta}' \bar{\varphi} + z_0) \\ \epsilon &= \frac{z - \hat{z}}{m_s^2} \end{aligned}$$

where $\rho(t)$ and $\bar{\vartheta}(t)$ are the estimates of ρ^* and $\bar{\vartheta}^*$ respectively, at time t and where m_s is designed to bound $\hat{\varphi}$, z_0 from above. An example of m_s with this property is $m_s^2 = 1 + \varphi' \varphi + z_0^2$. Let us consider the cost

$$J(\rho(t), \bar{\vartheta}(t)) = \frac{\epsilon^2 m_s^2}{2} = \frac{(z - \rho^* \bar{\vartheta}' \bar{\varphi} - \rho \xi + \rho^* \xi - \rho^* z_0)^2}{2 m_s^2} \quad (14)$$

where

$$\xi = \bar{\vartheta}' \bar{\varphi} + z_0 \quad (15)$$

Applying the gradient method, the following estimation law is obtained

$$\begin{aligned} \dot{\theta} &= \Gamma_1 \nabla J_\theta = \Gamma_1 \epsilon \rho^* \bar{\varphi} \\ \dot{\rho} &= \gamma \nabla J_\rho = \gamma \epsilon \xi \end{aligned} \quad (16)$$

where $\Gamma_1 = \Gamma_1' > 0$ and $\gamma > 0$ are the adaptation gains. Since ρ^* is not measurable, exploit the relation

$$\Gamma_1 \rho^* = \Gamma_1 |\rho^*| \text{sgn}(\rho^*) = \Gamma \rho^*$$

to obtain

$$\begin{aligned} \dot{\vartheta} &= \Gamma_1 \epsilon \text{sgn}(\rho^*) \bar{\varphi} \\ \dot{\rho} &= \gamma \epsilon \xi \\ \epsilon &= \frac{z - \rho \xi}{m_s^2}, \quad \xi = \bar{\vartheta}' \bar{\varphi} + z_0 \end{aligned} \quad (17)$$

The proof for convergence of the estimation error to zero is based on the Lyapunov function

$$V = \frac{\bar{\vartheta}' \Gamma^{-1} \bar{\theta}}{2} |\rho^*| + \frac{\bar{\rho}^2}{2 \gamma} |\rho^*| \quad (18)$$

where $\bar{\vartheta} = \bar{\vartheta} - \bar{\vartheta}^*$ and $\bar{\rho} = \rho - \rho^*$ are the parameter estimation errors.

Remark 2. The estimator (17) gives a simple tool to estimate both $\frac{1}{m_w(t)}$ and the parameters of the efficiency curve. Non-faulty data must be collected in order to estimate the non-faulty (nominal) values of efficiency and mass flow, call them $\bar{\vartheta}_{nom}^*$ and $\bar{\rho}_{nom}^*$. These data can be collected in the very first days of boiler operations. Once the nominal values have been estimated, the parameter estimator (17) will run in real time, and the estimated values will be compared with the nominal ones. Faults will be notified whether one of the following conditions are satisfied:

$$\text{if } \frac{\|\bar{\vartheta}'_{nom} \bar{\phi}(P_{in}, T_{rw}) - \bar{\vartheta}' \bar{\phi}(P_{in}, T_{rw})\|}{\|\bar{\vartheta}'_{nom} \bar{\phi}(P_{in}, T_{rw})\|} > t_{h_{eff}},$$

then \Rightarrow efficiency degradation

$$\text{if } \frac{\|\bar{\rho}_{nom} - \bar{\rho}\|}{\|\bar{\rho}_{nom}\|} > t_{h_{mass}},$$

then \Rightarrow mass flow change of working point

A practical way to select $t_{h_{eff}}$ and $t_{h_{mass}}$ is the following: $t_{h_{eff}} = 0.05$ would allow one to detect changes above 5% from the nominal point (maintenance is usually suggested when efficiency is reduced by 5% from the nominal case [37]). Similarly, having $t_{h_{mass}} = 0.05$ would be able to detect deviations above 5% from the nominal mass flow rate. Note that detection efficiency plays an important role: one would like to identify degradation as fast as possible (i.e. having a small $t_{h_{eff}}$ or $t_{h_{mass}}$). On the other hand, the presence of noise, which cannot be neglected in practice, would make it preferable to select slightly higher thresholds in order to avoid detection of false degradation.

Remark 3. By estimating the mass flow rate inside the boiler, the proposed bimodal estimation scheme (17) can be used not only for efficiency monitoring, but also for circulation pump monitoring. The estimated mass flow rate can be compared with the pump velocity or the mass flow rate estimated at the pump side to check whether water is not running properly, e.g. due to loss of pressure. One of the most common reasons for a condensing boiler to fail to provide heat is due to loss of pressure: loss of pressure can cause cavitation in the pump and thus has to be detected.

4. Actuator faults

For the detection of actuator faults, let us rearrange (9) as follows

$$\dot{\tilde{T}}_{sw}(t) = A\tilde{T}_{sw}(t) + B(\tilde{P}_{out}(t) + f_a(t)) + L\tilde{T}_{rw}(t) \quad (19)$$

where the matrices A, B, L are defined as

$$A = -\frac{m_w}{\rho_w V_b}, \quad B = \frac{1}{c_w \rho_w V_b}, \quad L = \frac{m_w}{\rho_w V_b} \quad (20)$$

Furthermore, $\tilde{T}_{sw} = T_{sw} - T_{sw}^{set}$, $\tilde{T}_{rw} = T_{rw} - T_{rw}^{eq}$, $\tilde{P}_{out} = P_{out} - P_{out}^{eq}$, where the equilibrium values satisfy

$$0 = A\tilde{T}_{sw}^{set}(t) + B\tilde{P}_{out}^{eq}(t) + L\tilde{T}_{rw}^{eq}(t) \quad (21)$$

Notice that the boiler is composed of an actuator (burner, cf. Fig. 3): this component is subjected to faults, malfunctioning and in general anything can cause a degradation of nominal performance.

The problem of fault detection in control systems is of utmost importance because it allows.

- The prompt detection of the fault, or even real-time detection in such a way to avoid permanent damage to the system.
- The development of fault tolerant control systems that can avoid a loss of performance.

Many unified term for such tasks have been coined, going from fault detection and isolation (FDI) to fault detection and diagnosis (FDD) [42]: the second one, which is also the most common in building automation, will be used within this work. It is also well-known that a typical approach to FDD relies on *analytical redundancy*: instead of replicating actuators and sensors (to check whether faults are present), the idea is to develop a mathematical model that from measured data can create a signal, the so-called *residual*, that helps in the fault diagnosis. The aim of fault detection and diagnosis is twofold:

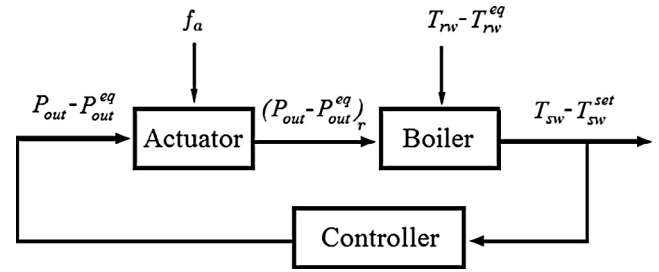


Fig. 3. Boiler, actuator and control system.

- *Residual generation*: generate a signal indicating the occurrence of a fault through the analysis of the information available in the system. The residual should be zero or small when no faults occur, while it should be not negligible in the presence of faults.
- *Decision*: the residual is analyzed via a decision rule, which determines the occurrence of a certain fault. The decision rule could be based on a comparison between a threshold and the instantaneous value of the residual, or based on a statistical decision method.

Actuator fault is modeled as additive fault

$$\tilde{P}_{out,r}(t) = \tilde{P}_{out}(t) + f_a(t)$$

where $\tilde{P}_{out,r}$ stands for the real input provided to the plant.

4.1. Fundamental limitations for detectability and isolability of faults

From a practical point of view, it might be relevant to consider not only actuator faults, but also sensor faults. In the following it is explained how, under assumptions A1–A3, there are fundamental limitations in the detection and isolation of multiple faults in condensing boilers. Let us consider a slightly more complex model than (9). In particular, the boiler is divided in three layers, and the heat transfer from one layer to the other is modeled as

$$\begin{aligned} \frac{c_w \rho_w V_b}{3} \dot{\tilde{T}}_{sw_1}(t) &= \tilde{P}_{out}(t) + f_a(t) - c_w m_w (\tilde{T}_{sw_1}(t) - \tilde{T}_{sw_2}(t)) \\ \frac{c_w \rho_w V_b}{3} \dot{\tilde{T}}_{sw_2}(t) &= -c_w m_w (\tilde{T}_{sw_2}(t) - \tilde{T}_{sw_3}(t)) - c_w m_w (\tilde{T}_{sw_2}(t) - \tilde{T}_{sw_1}(t)) \\ \frac{c_w \rho_w V_b}{3} \dot{\tilde{T}}_{sw_3}(t) &= -c_w m_w (\tilde{T}_{sw_3}(t) - \tilde{T}_{rw}(t)) - c_w m_w (\tilde{T}_{sw_3}(t) - \tilde{T}_{sw_2}(t)) \\ \tilde{T}_{sw}(t) &= \tilde{T}_{sw_1}(t) + f_s(t) \end{aligned} \quad (22)$$

where $\tilde{T}_{sw_1}, \tilde{T}_{sw_2}, \tilde{T}_{sw_3}$ refer to the deviation of the temperature of the boiler water from the equilibrium in each one of the three layers of the boiler, respectively. In (22) layer 1 is the closest one to the supply water and layer 3 is the closest one to the return water. The measured output, possibly affected by a fault, is the state of layer 1. It is desirable to detect and isolate the faults f_a and f_s (i.e. both the actuator and the temperature sensor for the supply water can be faulty). For easiness of notation let us rewrite the system in the compact form

$$\begin{aligned} \dot{\tilde{T}}_{sw,r}(t) &= A\tilde{T}_{sw,r}(t) + B(\tilde{P}_{out}(t) + f_a(t)) + L\tilde{T}_{rw}(t) \\ \tilde{T}_{sw}(t) &= C\tilde{T}_{sw,r}(t) + f_s(t) \end{aligned} \quad (23)$$

where $\tilde{T}_{sw_1}, \tilde{T}_{sw_2}, \tilde{T}_{sw_3}$ refer to the deviation of the with $\tilde{T}_{sw,r} = [\tilde{T}_{sw_1} \tilde{T}_{sw_2} \tilde{T}_{sw_3}]$ and the subscript r is used to denote the real state of the plant (possibly affected by a fault). The matrices in (23) are

$$A = \begin{bmatrix} -\frac{m_w}{3\rho_w V_b} & \frac{m_w}{3\rho_w V_b} & 0 \\ \frac{m_w}{3\rho_w V_b} & -\frac{m_w}{3\rho_w V_b} & \frac{m_w}{3\rho_w V_b} \\ 0 & \frac{m_w}{3\rho_w V_b} & -2\frac{m_w}{3\rho_w V_b} \end{bmatrix}, \quad B = \begin{bmatrix} \frac{1}{3c_w \rho_w V_b} \\ 0 \\ 0 \end{bmatrix}$$

$$L = \begin{bmatrix} 0 \\ 0 \\ \frac{m_w}{3\rho_w V_b} \end{bmatrix}, \quad C = [1 \quad 0 \quad 0] \quad (24)$$

The sensor fault can be modeled as a "pseudo actuator fault", if it exists a matrix F_{pa} such that

$$CF_{pa} = 1 \quad (25)$$

which allows the transformation $T_{sw} = C(\bar{T}_{swr} + F_{pa}f_s) = CU_{swr}$ and

$$\begin{cases} \dot{U}_{swr}(t) = AU_{swr}(t) + B(\bar{P}_{out}(t) + f_a(t)) + L\bar{T}_{rw}(t) + F_{pa}\dot{f}_s(t) - AF_{pa}f_s(t) \\ T_{sw}(t) = CU_{swr}(t) \end{cases}$$

Note that, given C in (24), the following matrix satisfies (25)

$$F_{pa} = \begin{bmatrix} 1 \\ 1 \\ 1 \end{bmatrix} \quad (26)$$

Thus, the sensor fault can be substituted by a pseudo-actuator fault through the linear map $[F_{pa} - AF_{pa}]$ in the new state variable U_{swr} .

It is now useful to introduce concepts to check whether a fault is actually detectable, or whether two faults can be isolated. These conditions are called conditions for detectability and isolability and are similar to the conditions for observability [42]. Consider the linear time invariant system

$$\begin{cases} \dot{U}_{swr}(t) = AU_{swr}(t) + Ff(t) \\ T_{sw}(t) = CU_{swr}(t) \end{cases}$$

where

$$F = [F_1 \quad F_2 \quad F_3] = [B \quad -F_{pa} \quad AF_{pa}]$$

after the pseudo-actuator transformation. The vector $f = [f_a \quad \dot{f}_s \quad f_s]$ is said to be observable from T_{sw} if and only if

$$\text{rank} \begin{bmatrix} CF \\ CAF \\ \dots \\ CA^{n-1}F \end{bmatrix} = m \quad (27)$$

where $m = 3$ is the dimension of the vector f . The fault f is detectable if and only if f is observable from T_{sw} . This condition is verified for A and F as in (24) and (27). Consider now the linear time invariant system

$$\begin{cases} \dot{U}_{swr}(t) = AU_{swr}(t) + F_1 f_a(t) + F_2 \dot{f}_s(t) + F_3 f_s(t) \\ T_{sw}(t) = CU_{swr}(t) \end{cases}$$

The faults are said to be isolable if and only if

$$\text{rank} [CA^{k_1}F_1 \quad CA^{k_2}F_2 \quad CA^{k_3}F_3] = 3 \quad (28)$$

where k_i are the smallest integers such that $CA^{k_i}F_i \neq 0$. Since $k_1 = 1, k_2 = 3$ and $k_3 = 2$, but (28) is not satisfied (in particular the rank is equal to 1), the conclusion is that the sensor and the actuator faults can be detected but cannot be isolated in the current setting, because of the structural properties of the system. A way to overcome such structural limitations is to add extra sensors for the temperature inside the boiler, e.g. for T_{sw_2} and T_{sw_3} . This would result in

$$C = \begin{bmatrix} 1 & 0 & 0 \\ 0 & 1 & 0 \\ 0 & 0 & 1 \end{bmatrix} \quad (29)$$

that would make the faults isolable. Unfortunately, in current boilers, only supply and return water can be measured, while no internal temperatures are measured. The proposed detectability and isolability analysis show that fault detection and diagnosis tools would definitely be enhanced if additional water temperature sensors were placed inside the boiler. This is further shown in Section 6.1, where isolability is shown if multiple sensors are present.

4.2. Residual generator

Since isolability of actuator and sensor faults is structurally not possible, the focus is on the system

$$\dot{\tilde{T}}_{sw}(t) = A\tilde{T}_{sw}(t) + B(\bar{P}_{out}(t) + f_a(t)) + L\bar{T}_{rw}(t) \quad (30)$$

with actuator fault only. The boiler is also subject to the process disturbance \bar{T}_{rw} (which is measurable).

The next step requires the development of a residual that is zero (or close to zero) when no fault acts on the system, and is different than zero when a fault is present. Consider the architecture of Fig. 4. A simple linear analysis reveals that

$$\tilde{T}_{sw}(s) = G(s)\bar{P}_{out}(s) + G_f(s)f_a(s) + G_d(s)\bar{T}_{rw}(s)$$

where

$$G(s) = (sI - A)^{-1}B$$

$$G_f(s) = (sI - A)^{-1}F$$

$$G_d(s) = (sI - A)^{-1}L$$

where $F = B$ and

$$\begin{aligned} r(s) &= H_d(s)\bar{T}_{rw}(s) + H_y(s)\tilde{T}_{sw}(s) - H_u(s)\bar{P}_{out}(s) \\ &= (H_y(s)G(s) - H_u(s))\bar{P}_{out}(s) + H_y(s)G_f(s)f(s) + (H_d(s) \\ &\quad + H_y(s)G_d(s))\bar{T}_{rw}(s) \end{aligned} \quad (31)$$

For a perfectly working residual, it is desirable that

$$\begin{cases} r(s) = 0 & \text{if } f(s) = 0 \\ r(s) \neq 0 & \text{if } f(s) \neq 0 \end{cases} \quad (32)$$

Ideally, this is satisfied if

$$\begin{cases} H_y(s)G_d(s) + H_d(s) = 0 \\ H_y(s)G(s) - H_u(s) = 0 \end{cases} \quad (33)$$

5. Actuator and sensor faults

The relations (33) can be quite conservative to be achieved. In order to relax them, and to relax the isolability conditions to 'quasi' isolability, consider the norm condition

$$\begin{cases} \|H_y(s)G_d(s) + H_d(s)\|_2 \leq \gamma_1 \\ \|H_y(s)G(s) - H_u(s)\|_2 \leq \gamma_2 \end{cases} \quad (34)$$

with the objective to determine $H_y(s), H_u(s)$ and $H_d(s)$ in such a way that the L_2 norm is minimized (alternatively, L_1 or L_∞ norms can be considered). Let us consider the system with both actuator and sensor fault

$$\begin{cases} \dot{\tilde{T}}_{swr}(t) = A\tilde{T}_{swr}(t) + B(\bar{P}_{out}(t) + f_a(t)) + L\bar{T}_{rw}(t) \\ \tilde{T}_{swr}(t) = \tilde{T}_{sw}(t) + f_s(t) \end{cases} \quad (35)$$

Let us consider the two residual generators

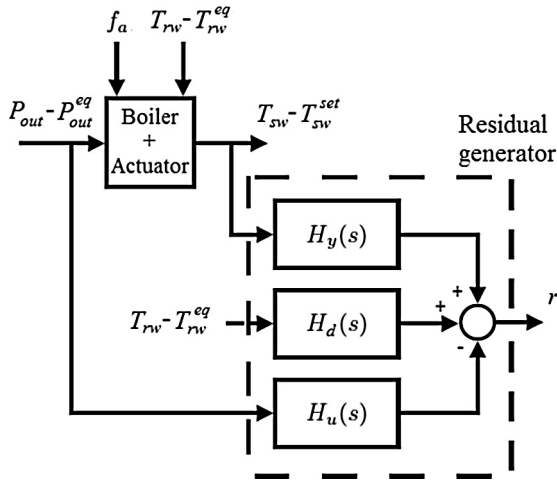


Fig. 4. Residual generator.

$$\begin{cases} \dot{\hat{T}}_{sw_a}(t) = A\hat{T}_{sw_a}(t) + B\bar{P}_{out}(t) + L\bar{T}_{rw}(t) + K_a(\bar{T}_{sw_a}(t) - \hat{T}_{sw}(t)) \\ r_a(t) = \bar{T}_{sw_a}(t) - \hat{T}_{sw}(t) \end{cases} \quad (36)$$

$$\begin{cases} \dot{\hat{T}}_{sw_s}(t) = A\hat{T}_{sw_s}(t) + B\bar{P}_{out}(t) + L\bar{T}_{rw}(t) + K_s(\bar{T}_{sw_s}(t) - \hat{T}_{sw}(t)) \\ r_s(t) = \bar{T}_{sw_s}(t) - \hat{T}_{sw}(t) \end{cases} \quad (37)$$

where K_a and K_s are the observer gains to be designed such that $(A - K_a C)$ and $(A - K_s C)$ are asymptotically stable. Note that the disturbance T_{rw} can be measured, so it can be included in the observer. The gain K_a is synthesized in such a way that the following Kalman filtering problem is solved

$$\begin{aligned} & \min_{K_a} \lim_{t \rightarrow \infty} E\{r'_a(t)r_a(t)\} \\ & \text{s.t.} \\ & E\{f_a(t)f'_a(\tau)\} = \delta(t - \tau)I \\ & (A - K_a C) \text{ is asymptotically stable} \end{aligned} \quad (38)$$

The gain K_s is synthesized in such a way that the following Kalman filtering problem is solved

$$\begin{aligned} & \min_{K_s} \lim_{t \rightarrow \infty} E\{r'_s(t)r_s(t)\} \\ & \text{s.t.} \\ & E\{f_s(t)f'_s(\tau)\} = \delta(t - \tau)I \\ & (A - K_s C) \text{ is asymptotically stable} \end{aligned} \quad (39)$$

Notice that (38) minimizes the effect of f_s on r_a in terms of the L_2 norm (quasi-isolability of actuator fault), while (39) minimizes the effect of f_a on r_s in terms of the L_2 norm (quasi-isolability of sensor fault). The overall fault detection and diagnosis architecture, comprising of efficiency/mass flow estimator (17), and actuator/sensor faults residual generators (38), (39) is shown in Fig. 5. Notice that since P_{out} is not directly measurable, it has to be estimated via the bimodal estimator (17).

Remark 4. Instead of comparing T_{sw} with T_{sw}^{set} (static strategy), the residual generators (36) and (37) boil down to comparing the state of the filter \hat{T}_{sw} with the state of the system \bar{T}_{sw} (dynamic strategy). In such a way, also the transient dynamics are considered. At steady-state, without faults, both the static and the dynamic strategy will converge to the same result: however the dynamic strategy has the merit of considering the whole operational envelope of the boiler (not only the steady-state-operation). Note that the changing of operating conditions may lead to the change of control commands and actuator position: however, this is not a

problem for the proposed FDD scheme, as soon as the efficiency and mass flow estimators converge. In fact, what the estimators in Fig. 5 are doing is to linearize the system around the new working point, so that normal transferring of operation conditions will not affect fault detection.

Remark 5. Similarly to the thresholds for efficiency and mass flow degradation, it is possible to define some thresholds for detecting actuator and sensors faults. For example:

$$\begin{aligned} & \text{if } E\{r'_a r_a\} > t_{h_a}, \text{ then } \Rightarrow \text{actuator fault} \\ & \text{if } E\{r'_s r_s\} > t_{h_s}, \text{ then } \Rightarrow \text{sensor fault} \end{aligned} \quad (40)$$

A practical way to select t_{h_a} and t_{h_s} is the following: the norm of the residuals is upper bounded by $\|H_{f_a-r_a}\|_2^2 E\{f'_a f_a\}$ and $\|H_{f_s-r_s}\|_2^2 E\{f'_s f_s\}$, where $H_{f_a-r_a}(s)$ and $H_{f_s-r_s}(s)$ are the transfer functions between the fault and the corresponding residual. By selecting, e.g. $t_{h_a} = 0.1 \|H_{f_a-r_a}\|_2^2$ and $t_{h_s} = 0.1 \|H_{f_s-r_s}\|_2^2$ one would not be able to detect faults whose covariance is smaller than 0.1.

Since the L_2 norm might be conservative, a more practical direction is to measure $E\{r'_{anom} r_{anom}\}$ and $E\{r'_{snom} r_{snom}\}$, where r_{anom} and r_{snom} are the residuals in the nominal case (e.g. from data collected during non-faulty operation). Then by normalizing the expression in (40) with the norm of the residual during non-faulty operation

$$\begin{aligned} & \text{if } \frac{E\{r'_a r_a\}}{E\{r'_{anom} r_{anom}\}} > t_{h_a}, \text{ then } \Rightarrow \text{actuator fault} \\ & \text{if } \frac{E\{r'_s r_s\}}{E\{r'_{snom} r_{snom}\}} > t_{h_s}, \text{ then } \Rightarrow \text{sensor fault} \end{aligned} \quad (41)$$

one would be able to detect percentage variations with respect to the nominal case. Note that, similar to Remark 2, detection efficiency plays an important role: one would like to identify faults as fast as possible (i.e. having a small t_{h_a} or t_{h_s}). On the other hand, the presence of noise, which cannot be neglected in practice, would make it preferable to select slightly higher thresholds in order to avoid detection of false faults.

Remark 6. Sensor noise might degrade the performance of residual generators. For example, a noise acting on the sensor temperature, will have the same effect of a possible fault. This issue can be solved by noticing that faults act mainly at low frequencies, while sensor noise acts at high frequency. Adding appropriate pass band filters in the synthesis of (38) and (39) will help decoupling the effect of noise from the effect of faults.

6. Results

In this section the proposed monitoring methods are extensively tested on a boiler model obtained via the approach in [43]. The simulation run in Matlab R2014a in a workstation with quad-core processor at 3.6 GHz, 10 MB cache, RAM 8 GB at 1600 MHz. The modeling approach in [43] was selected thanks to its capability to approximate very accurately real-life boilers: this approach avoids the static nonlinear efficiency curve and accounts for a time-varying proportion of dry/wet heat exchange. Basically the model in [43] coincides with the model in Fig. 2 at steady state, while allowing for a richer dynamical behavior.³ At steady state, the model in Fig. 2 is basically approximately equal to the model in [40].

³ Note that, due to its richer complexity, real-time monitoring energy efficiency and performance degradation of condensing boilers modeled via [33] is still an open problem.

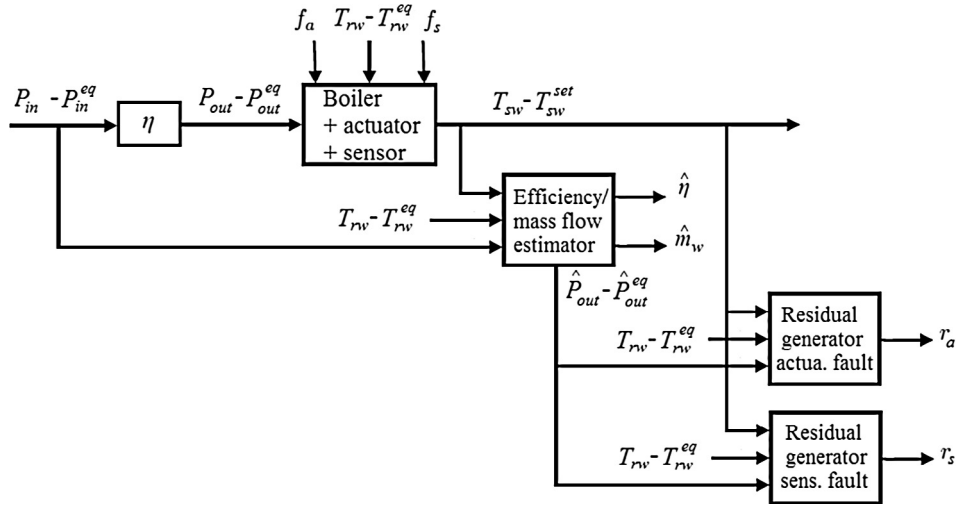


Fig. 5. Proposed fault detection and diagnosis architecture.

There, a two-node thermal model is adopted to model the relation between heat input and temperature of return water. The combustion process is not modeled explicitly, but via a boiler efficiency characteristic as follows

$$\eta(P_{in}, T_{rw}) = a_1 T_{rw} + a_2 T_{rw}^2 + a_3 T_{rw}^3 + a_4 T_{rw}^4 + a_5 L + a_6 T_{rw} L + a_7 T_{rw}^2 L + a_8 \quad (42)$$

where L is the boiler load normalized between 0 and 1. In our case, L is calculated with respect to the gas side instead of the water side. A model and a curve as in (42) is then fitted and validated so as to match the behavior of real operating boilers (using system identification as explained in [43]).

The following curve is obtained:

$$\begin{aligned} a_1 &= 8.841 & a_5 &= 12.024 \\ a_2 &= -0.2564 & a_6 &= 0.2710 \\ a_3 &= 3.945 \cdot 10^{-3} & a_7 &= 1.230 \cdot 10^{-3} \\ a_4 &= -1.7983 \cdot 10^{-5} & a_8 &= 7.147 \end{aligned} \quad (43)$$

which is shown in Fig. 6 for different loads (full load (100%), half load (50%), part load (20%)). Fig. 6 shows also the approximation of the efficiency curve via the bimodal estimator (17). It can be observed that the bimodal description is a good approximation of the efficiency curve. The nominal efficiency curve undergoes now a degradation, and the online estimator runs till convergence to the new parameters. It can be seen from Fig. 7 that a good agreement is obtained, which means that the proposed estimator is able to track degradation of performance.

The online performance of the proposed bimodal estimator is now shown. In Fig. 8 it is possible to recognize two phases. In the first phase ($t < 50$ min) the boiler is perfectly functioning: performance curve and mass flow are initially unknown, so that a learning period is necessary before converging to the real values. In the second phase ($t > 50$ min) the boiler undergoes a degradation and at the same time the mass flow rate moves from its nominal value. The estimator is able to track the degradation in real-time, and at the same time also the correct mass flow rate is estimated.

Actuator and sensor fault detection and isolation is now tested: the two Kalman filters designed as in (38) and (39) are implemented. An actuator fault occurs at 350 s, while a sensor fault occurs at 550 s. The actuator fault is taken as a multiplicative fault, $f_a = -0.2\hat{P}_{out}$, i.e. the actuator loses 20% of its efficiency: the sensor fault is taken as a multiplicative fault, $f_s = -0.1\hat{T}_{sw1}$, i.e. the sensor

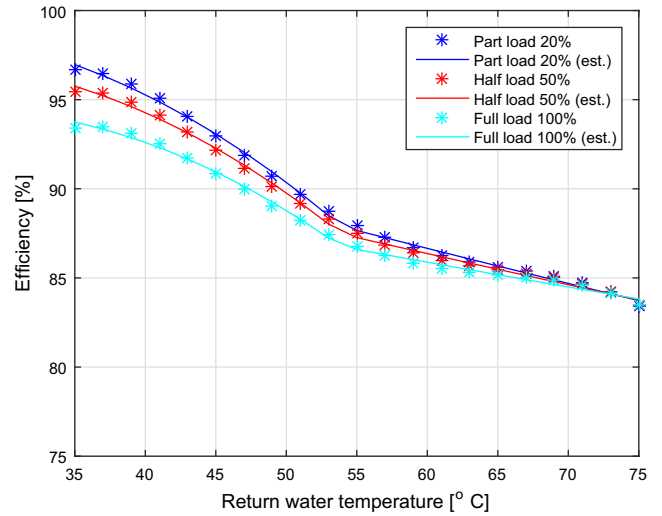


Fig. 6. Efficiency curve in nominal conditions: real curve (stars) and estimated curve (solid).

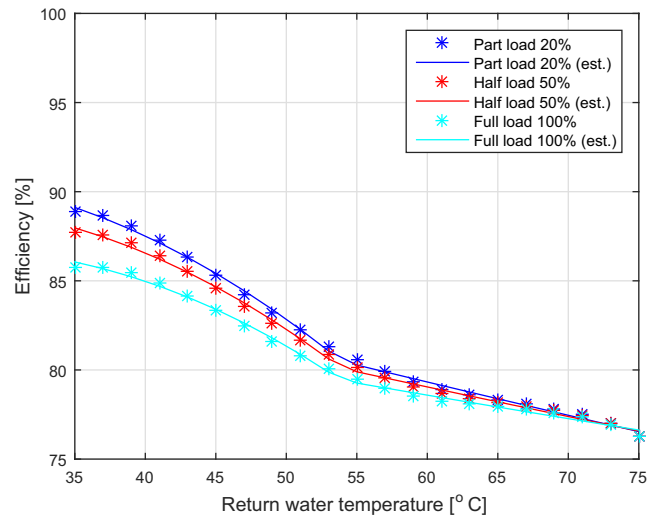


Fig. 7. Efficiency curve in degraded conditions: real curve (stars) and estimated curve (solid).

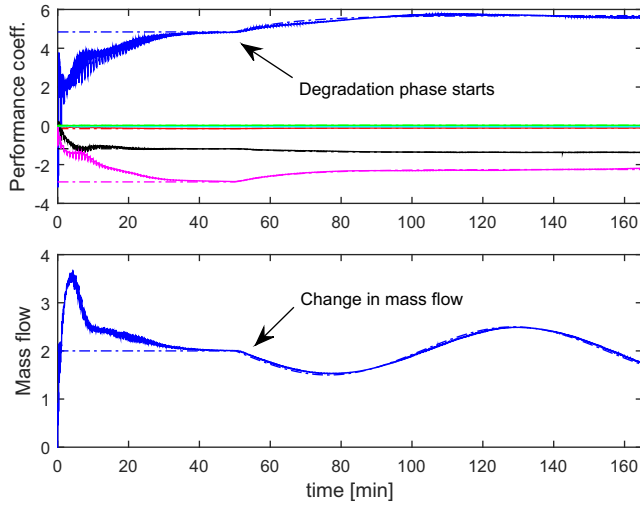


Fig. 8. Performance coefficients and mass flow: real values (dash-dot) and estimated values (solid).

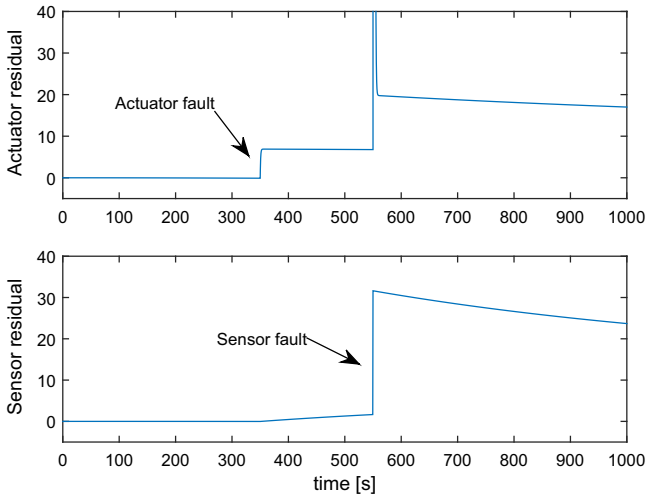


Fig. 9. Residual for actuator and sensor faults: actuator fault at 350 s, sensor fault at 550 s.

generates a bias since it decreases its readings by 10%. Fig. 9 reveals that both faults are correctly detected. However, due to the structural limitations, they cannot be perfectly isolated. In fact, notice that the sensor residual generator is slightly activated starting from 350 s, while the actuator residual presents a spike at 700 s, followed by a slowly decreasing bias.

6.1. Perfect fault isolation in the case of multiple sensor measurements

It has been shown that it is not possible to perfectly isolate actuator and sensor faults if only one temperature is measured. Perfect isolation can occur if multiple measurements are available for water temperature across the boiler. Let us consider the system

$$\begin{aligned} \dot{\bar{T}}_{sw_r}(t) &= A\bar{T}_{sw_r}(t) + B(\bar{P}_{out}(t) + f_a(t)) + L\bar{T}_{rw}(t) \\ \bar{T}_{sw}(t) &= \bar{T}_{sw_r}(t) + Ef_s(t) \end{aligned} \quad (44)$$

with A, B and L has in (24), and

$$E = \begin{bmatrix} 1 \\ 0 \\ 0 \end{bmatrix} \quad (45)$$

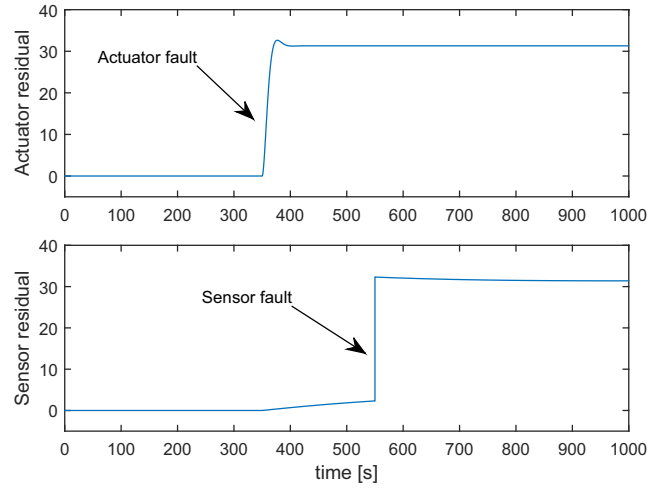


Fig. 10. Residual for actuator and sensor faults (with perfect isolation): actuator fault at 350 s, sensor fault at 550 s.

so as to consider a possible fault in the first sensor. The sensor fault is taken as a multiplicative fault, $f_s = -0.1\bar{T}_{sw_1}$ as in the previous case. By defining the matrix $Q = I - EE^+$, with $E^+ = (E'E)^{-1}E'$ and the observer

$$\begin{aligned} \dot{\hat{T}}_{sw_r}(t) &= A\hat{T}_{sw_r}(t) + B\hat{P}_{out}(t) + L\hat{T}_{rw}(t) + KQ(y(t) - \hat{y}(t)) \\ r(t) &= Q(\bar{T}_{sw}(t) - \hat{T}_{sw_r}(t)) = Q(\bar{T}_{sw_r}(t) - \hat{T}_{sw_r}(t)) + QEf_s(t) \\ &= Q(\bar{T}_{sw_r}(t) - \hat{T}_{sw_r}(t)) \end{aligned} \quad (46)$$

it is concluded that the residual r is not influenced by the sensor fault f_s , which allows perfect isolation of the actuator fault. Under the same fault scenario (actuator fault at 350 s, sensor fault at 550 s), Fig. 10 shows how the actuator fault is now perfectly isolated and the respective residual is not influenced by the sensor fault at 550 s.

7. Conclusions

Condensing boilers are becoming more and more adopted and many countries have encouraged the use of condensing boilers with financial incentives. It is thus important to develop software tools to assess the correct functioning of the boiler and eventually detect problems. The bimodal behavior of the boiler (condensing/noncondensing mode) makes the development of these tools non-trivial. This work developed a fully-fledged set of fault detection and diagnosis tools for condensing boilers. The tools have been organized as follows: a bimodal parameter estimator to detect deviations of the efficiency of the boiler from nominal values in both condensing and noncondensing mode; a virtual sensor for the estimation of the water mass flow rate; filters to detect actuator and sensor faults, possibly due to control and sensing problems. Interesting structural properties for detection and isolation of actuators and sensing faults have been derived. In particular it was shown that additional water temperature sensors are useful to isolate actuator and sensor faults. The effectiveness of these tools was verified via extensive simulations.

Acknowledgments

The research leading to these results has been partially funded by the Marie-Curie call FP7-PEOPLE-2012-IAPP 'Advanced Methods for Building Diagnostics and Maintenance' (AMBI). The work of Le Quang Thuan is partially funded by Vietnam National Foundation

for Science and Technology Development (NAFOSTED) under Grant No. 101.02-2014.32

References

- [1] Pérez-Lombard L, Ortiz J, Pout C. A review on buildings energy consumption information. *Energy Build* 2008;40(3):394–8.
- [2] Bonvini M, Sohn MI D, Granderson J, I Wetter M, Piette MA. Robust on-line fault detection diagnosis for HVAC components based on nonlinear state estimation techniques. *Appl Energy* 2014;124:156–66.
- [3] Michailidis IT, Baldi S, Kosmatopoulos EB, Boutalis YS. Optimization-based active techniques for energy efficient building control part II: Real-life experimental results. In: International conference on buildings energy efficiency and renewable energy sources, BEE RES 2014, p. 39–42.
- [4] Central Heating System Specifications. Domestic heating by gas: boiler systems guidance for installers and specifiers. Energy Saving Trust; 2008.
- [5] Lazzarin RM. Condensing boilers in buildings and plants refurbishment. *Energy Build* 2012;47:61–7.
- [6] Holub O, Macek K. HVAC simulation model for advanced diagnostics. In: 2013 IEEE 8th international symposium on intelligent signal processing (WISP).
- [7] Lee S, Kum S-M, Lee C-E. Performances of a heat exchanger and pilot boiler for the development of a condensing gas boiler. *Energy* 2011;36:3945–51.
- [8] Lee S, Kum S-M, Lee C-E. An experimental study of a cylindrical multi-hole premixed burner for the development of a condensing gas boiler. *Energy* 2011;36:4150–7.
- [9] Lee C-E, Yu B, Lee S. An analysis of the thermodynamic efficiency for exhaust gas recirculation-condensed water recirculation-waste heat recovery condensing boilers (EGR-CWR-WHR CB). *Energy* 2015;86:267–75.
- [10] Che D, Liu Y, Gao C. Evaluation of retrofitting a conventional natural gas fired boiler into a condensing boiler. *Energy Convers Manage* 2004;45:3251–66.
- [11] Chen Q, Finney K, Li H, Zhang X, Zhou J, Sharifi V, et al. Condensing boiler applications in the process industry. *Energy Build* 2012;89:30–6.
- [12] Vigants G, Galindoms G, Veidenbergs I, Vigants E, Blumberga D. Efficiency diagram for district heating system with gas condensing unit. *Energy Procedia* 2015;72:119–26.
- [13] Underwood CP, Yik FWH. Modelling methods for energy in buildings. Blackwell Publishing Ltd; 2004.
- [14] Rosa L, Tosato R. Experimental evaluation of seasonal efficiency of condensing boilers. *Energy Build* 1990;14:237–41.
- [15] Jeong K, Kessen MJ, Bilirgen H, Levy EK. Analytical modeling of water condensation in condensing heat exchanger. *Int J Heat Mass Transfer* 2010;53:2361–8.
- [16] Di Perna C, Magri G, Giuliani G, Serenelli G. Experimental assessment and dynamic analysis of a hybrid generator composed of an air source heat pump coupled with a condensing gas boiler in a residential building. *Appl Therm Eng* 2015;76:86–97.
- [17] Naumchik IV, Kinzhagulov IY, Kren P, Stepanova. Mass flow meter for liquids. *Sci Tech J Inform Technol Mech Opt* 2015;15:900–6.
- [18] Karnouskos S, Havlena V, Jerhotova E, Kodet P, Sikora M, Stluka P, et al. Plant energy management. *Ind Cloud-Based Cyber-Phys Syst* 2014:203–2018.
- [19] Taler Jan, Wglowski Bohdan, Taler Dawid, Sobota Tomasz, Dzierwa Piotr, Trojan Marcin, et al. Determination of start-up curves for a boiler with natural circulation based on the analysis of stress distribution in critical pressure components. *Energy* 2015;92(1):275–83.
- [20] Lazzarin R. The importance of the modulation ratio in the boilers installed in refurbished buildings. *Energy Build* 2014;75:43–50.
- [21] Baldi S, Michailidis IT, Ravanis C, Kosmatopoulos EB. Model-based and model-free plug-and-play building energy efficient control. *Appl Energy* 2015;154:829–41.
- [22] Parisio A, Rikos E, Tzamalīs G, Glielmo L. Use of model predictive control for experimental microgrid optimization. *Appl Energy* 2014;115:37–46.
- [23] Vivekananthan Cynthujah, Mishra Yateendra, Ledwich Gerard, Li Fangxing. Demand response for residential appliances via customer reward scheme. *IEEE Trans Smart Grid* 2014;5(2):809–20.
- [24] Wang Zhu, Wang Lingfeng, Dounis Anastasios I, Yang Rui. Multi-agent control system with information fusion based comfort model for smart buildings. *Appl Energy* 2012;99:247–54.
- [25] Xu Xiaojing, Culligan Patricia J, Taylor John E. Energy saving alignment strategy: achieving energy efficiency in urban buildings by matching occupant temperature preferences with a buildings indoor thermal environment. *Appl Energy* 2014;123:209–19.
- [26] Comodi G, Giantomassi A, Severini M, Squartini S, Ferracuti F, Fonti A, et al. Multi-apartment residential microgrid with electrical and thermal storage devices: experimental analysis and simulation of energy management strategies. *Appl Energy* 2015;137:854–66.
- [27] Mossolli M, Ghali K, Ghaddar N. Optimal control strategy for a multi-zone air conditioning system using a genetic algorithm. *Energy* 2009;34(1):58–66.
- [28] Tanaka Kenichi, Yoza Akihiro, Ogimi Kazuki, Yona Atsushi, Senjyu Tomonobu, Funabashi Toshihisa, et al. Optimal operation of DC smart house system by controllable loads based on smart grid topology. *Renewable Energy* 2012;39(1):132–9.
- [29] Baldi S, Karagevrekis A, Michailidis IT, Kosmatopoulos EB. Joint energy demand and thermal comfort optimization in photovoltaic-equipped interconnected microgrids. *Energy Convers Manage* 2015;101:352–63.
- [30] Wang Zhu, Yang Rui, Wang Lingfeng, Green RC, Dounis Anastasios I. A fuzzy adaptive comfort temperature model with grey predictor for multi-agent control system of smart building. In: 2011 IEEE Congress on Evolutionary Computation (CEC). IEEE; 2011. p. 728–35.
- [31] Hussain S, Gabbar HA, Bondarenko D, Musharavati F, Pokhare S. Comfort-based fuzzy control optimization for energy conservation in HVAC systems. *Appl Therm Eng* 2014;67:507–19.
- [32] Tzivanidis C, Antonopoulos KA, Gioti F. Numerical simulation of cooling energy consumption in connection with thermostat operation mode and comfort requirements for the athens buildings. *Appl Energy* 2011;88(8):2871–84.
- [33] Satyavada H, Babuska R, Baldi S. Integrated dynamic modelling and multivariable control of HVAC components. In: 15th European control conference, Aalborg, Denmark, June 29–July 1st, 2016. p. 1171–6.
- [34] Afram A, Janabi-Sharifi F. Review of modeling methods for HVAC systems. *Appl Therm Eng* 2014;67:507–19.
- [35] Bick V, Holub O, Marik K, Sikora M, Stluka P, Dhulst R. Platform for coordination of energy generation and consumption in residential neighborhoods. In: 2012 3rd IEEE PES innovative smart grid technologies Europe (ISGT Europe).
- [36] ClearFire condensing boiler operation, service, and parts. Cleaver Brooks; 2015.
- [37] O'Brien: energy engineered. Energy efficiency best practice guide: steam, hot water and process heating systems; 2009.
- [38] Boiler Guide; 2015. <<http://www.boilerguide.co.uk/articles/boiler-problems/top-10-most-common-boiler-problems>>.
- [39] American Society of Heating, Refrigerating and Air-Conditioning Engineers ASHRAE. ASHRAE handbook HVAC systems and equipment; 2016.
- [40] Cockroft J, Samuel A, Tuohy P. Development of a methodology for the evaluation of domestic heating controls. Phase 2 of a DEFRA Market Transformation Programme project, carried out under contract to BRE Environment. University of Strathclyde, Energy Systems Research Unit; 2007.
- [41] Thuan LQ, van den Boom T, Baldi S. Online identification of continuous bimodal and trimodal piecewise affine systems. In: 15th annual European Control Conference (ECC2016).
- [42] Isermann R. Fault-diagnosis systems: an introduction from fault detection to fault tolerance. Springer; 2006.
- [43] Satyavada H, Baldi S. A novel modelling approach for condensing boilers based on hybrid dynamical systems. *Machines* 2016;4:10.